Quaternary Science Reviews 71 (2013) 175–190

Contents lists available at SciVerse ScienceDirect

Quaternary Science Reviews

journal homepage: www.elsevier.com/locate/quascirev

Reconstruction of palaeoprecipitation based on pollen transfer functions – the record of the last 16 ka from Laguna Potrok Aike, southern Patagonia

Frank Schäbitz [a,*], Michael Wille [a], Jean-Pierre Francois [a], Torsten Haberzettl [b], Flavia Quintana [a,c], Christoph Mayr [d,e], Andreas Lücke [f], Christian Ohlendorf [g], Virginia Mancini [h], Marta M. Paez [h], Aldo R. Prieto [h], Bernd Zolitschka [g]

[a] Seminar für Geographie und ihre Didaktik, University of Cologne, Gronewaldstr. 2, D-50931 Cologne, Germany
[b] Physical Geography, Institute of Geography, University of Jena, Löbdergraben 32, D-07743 Jena, Germany
[c] Centro Regional Universitario Bariloche, Instituto de Investigaciones en Biodiversidad y Medioambiente, San Carlos de Bariloche, Argentina
[d] Institute of Geography, University of Erlangen-Nuremberg, Kochstr. 4/4, D-91054 Erlangen, Germany
[e] Institute of Paleontology and Geobiology, University of Munich, Richard-Wagner-Str. 10, D-80333 Munich, Germany
[f] Institute of Bio- and Geosciences, IBG-3: Agrosphere, Research Center Jülich, D-52425 Jülich, Germany
[g] GEOPOLAR, Institute of Geography, University of Bremen, Celsiusstr. FVG-M, D-28359 Bremen, Germany
[h] Laboratorio de Palinología, Universidad Nacional de Mar del Plata, Funes 3254, 7600 Mar del Plata, Argentina

A R T I C L E I N F O

Article history:
Received 14 December 2011
Received in revised form
5 November 2012
Accepted 11 December 2012
Available online 22 January 2013

Keywords:
ICDP-project PASADO
Modern pollen samples
Transfer function
Pollen
Precipitation reconstruction
Palaeoclimate
Late Quaternary
Southern Hemisphere Westerlies

A B S T R A C T

Based on modern pollen samples from different vegetation units in southern Patagonia, showing a close relation to yearly amounts of precipitation and mean annual temperatures, different pollen–climate transfer functions are developed and tested. Comparing the performance of MAT (Modern Analogue Techniques), WA (Weighted Average), as well as WAPLS (Weighted Average Partial Least Square) statistical techniques, it is possible to determine the statistically most robust model (WAPLS for precipitation). This transfer function is then used to estimate palaeoprecipitation amounts based on Laguna Potrok Aike pollen results for the last 16,000 years. Generally, the results of the precipitation model indicate less precipitation during the Lateglacial and alternating wet and dry periods during the Holocene. The Holocene started with higher amounts of precipitation until about 8 ka cal. BP, followed by a period with lower amounts between 8 and 2.5 ka cal. BP, while the Late Holocene shows a general increase in precipitation. Comparisons with former shoreline reconstructions and carbonate concentrations in the sediments of Laguna Potrok Aike not always show similarities due to the complex environmental factors recorded by these proxies. Moreover, changes in the moisture availability due to the interplay of precipitation and temperature, cannot be reconstructed directly. Nevertheless, the general long-term trend of palaeoprecipitation is in accordance with the absolute moisture content in the air, which is determined mainly by temperature: during cold periods with less absolute moisture, the model shows less precipitation. Moreover, the model also points to a relation with the position and strength of the Southern Hemisphere Westerlies.

1. Introduction

The present climate of the southern South American continent (Patagonia) is mainly influenced by the Southern Hemisphere west winds (SHW) and the topography of the landmass (Mayr et al., 2007a, 2007b). The eastern part is much semi-arid because of the rain shadow effect of the Andes and is covered by drought-resistant Patagonian steppe vegetation. In contrast, the Andes and the southwestern Chilean lowlands where the SHW arrive at the continent first are very wet due to orographic rainfall. The areas along the Chilean coast are covered by Nothofagus forests while in the westernmost, extremely wet fjord coast moorlands occur. Above the forest in the highest southern Andes grass dominated altoandine vegetation predominates. This strong ecological and climatic gradient has been investigated for the late Quaternary since nearly 70 years by numerous studies (e.g. Auer, 1946; Markgraf, 1993; Heusser, 1995; Haberzettl et al., 2005; Lamy et al., 2010; Moreno et al., 2010), using different archives (terrestrial, lacustrine and

* Corresponding author. Tel.: +49 221 4704630; fax: +49 221 4706736.
E-mail address: frank.schaebitz@uni-koeln.de (F. Schäbitz).

0277-3791/$ – see front matter © 2013 Elsevier Ltd. All rights reserved.
http://dx.doi.org/10.1016/j.quascirev.2012.12.006

marine) in order to understand their environmental settings in the past. Located close to the Antarctic continent, the Quaternary history of southernmost South America is connected to and triggered by the ice balance and climatic development of its neighbouring continent. Furthermore, Southern Patagonia is an important source region for dust particles found in Antarctic ice cores (Delmonte et al., 2008). To understand the transport mechanisms of these particles, reconstruction of the southern hemisphere wind belts throughout the Quaternary is crucial. Moreover, the outlined environmental setting of southern South America allows testing different hypothesis for the position and strength of the SHW by using proxy data from different archives.

Here we present the first pollen-based quantitative precipitation reconstruction for the drier eastern part of southern Patagonia using samples from the ICDP deep drilling site Laguna Potrok Aike at about 52° southern latitude. This reconstruction is based on the last 16 ka pollen data analysed with an average temporal resolution of 67 years (Wille et al., 2007). The main questions are (I) whether the statistical model is robust enough to be used for the reconstruction of late Pleistocene climate changes, (II) how the results compare to other important proxies from sediment cores of Laguna Potrok Aike, as well as (III) how these results relate to regional palaeoclimate studies. The palaeoprecipitation signal could further be used to detect and quantitatively describe dry and wet intervals during Quaternary times and to correlate them to deflation events in Patagonia, which were detected in Antarctic ice cores as prominent dust accumulation peaks. This could then be interpreted as a direct link between terrestrial and glacial archives on both southern hemispheric continents.

2. Regional setting

2.1. Site description

Laguna Potrok Aike has been monitored, cored and studied since 2001 (Schäbitz et al., 2003; Zolitschka et al., 2006). It is a volcanic maar located in the Pali Aike volcanic field at 52°S and 70°W at an elevation of 113 m asl about 80 km north of the Strait of Magellan (Fig. 1). The current maximal depth of the central water body is 100 m, but several terraces surrounding the lake document higher lake levels in the past (Haberzettl et al., 2007; Kliem et al., 2013b). As revealed by seismic studies palaeoshorelines also occur below the current water line and were formed by wave action (Haberzettl et al., 2008; Anselmetti et al., 2009; Gebhardt et al., 2011a, 2011b). Sediments of Laguna Potrok Aike were first cored (2002–2006) in the framework of the SALSA-project ("South Argentinean Lake Sediment Archives and modelling"). The cores were studied for sedimentological and biological proxies (Haberzettl et al., 2005, 2006, 2007, 2008, 2009; Wille et al., 2007; Mayr et al., 2007a, 2009).

2.2. Climate of Southern Patagonia

The modern climate of south-eastern Patagonia is characterized by dry with cool summers and mild winters (e.g., Schwerdtfeger, 1976; Endlicher, 1993) and mainly determined by the SHW belt (Fig. 2). Situated in the so-called "furious fifties" the yearly mean summer wind speed at 50°S is about 10 m/s (Weischet, 1996) and exceeds comparable situations at the same latitude in the Northern Hemisphere four times. Furthermore, the wind speed may rise from 1 h to the next by 140 km/h during intense storm events, which can happen throughout the year but occurs more frequently during summer times. For southern Patagonia the wind phenomenon is very important and influences all other climatic parameters considerably as well as the vegetational setting (i.e., deformation of trees) and the physiology of plants (reduced photosynthesis). Therefore, Weischet (1996) characterized this climate as "extremely wind dominated summer cool and winter mild". The wind is mainly the reason for (a) the cool temperature setting, (b) the high evaporation rate, (c) the extreme precipitation gradient from west to east, (d) the frequent and very fast changes in weather conditions, (e) the frequency of cyclonal activity and (f) the high vorticity. Generally, a total of twelve to fourteen vorticities originate in the SHW (Weischet, 1996). In combination with topography this results in a high diversity in regional and local sub-climates. The reason for such an extreme wind influence is the lack of landmasses in the southern latitudes between 40° and 60°S and the large ice mass on Antarctica which determines the high temperature and pressure gradient between the South Pole and the southern hemispheric subtropics (Schwerdtfeger, 1976; Weischet, 1996). This fixes the polar front and the centre of the zonal winds (Fig. 2) in summer between 50 and 40°S and in winter around 30°S (Moy et al., 2009). The seasonal position of the zonal winds also determines the main precipitation amounts, which are higher in southwest Patagonia during December to February (southern summer) while in northwest Patagonia the winter months (June to August) receive more precipitation. Furthermore, the cold katabatic winds descending from the Antarctic continent supply the subpolar southern latitudes with cold air, a wide spread seasonal sea ice cover (up to 60°S in the southwest Atlantic) and the Antarctic convergence zone between 48 and 45°S (Weischet, 1996). Because of preferred routes of these katabatic winds, one centre for the formation of cyclones is situated east of the Patagonian coast in the South-West Atlantic. The fronts of these cyclones are important for the weather on the southern tip of the South American continent (Endlicher, 1993; Moy et al., 2009). From time to time they also allow wet air masses coming in from the Atlantic to create extreme precipitation events in the eastern dry lands of southern Patagonia. These extreme events are in strong contrast to the precipitation supply to Laguna Potrok Aike from western and south-western wind directions (Fig. 3). Incoming air masses from westerly directions have to cross the Andean mountains, therefore loose considerable amounts of moisture at the western slopes in the Chilean part of South Patagonia and reach the eastern dry lands with only few to no precipitation left in form of a foehn wind system (Schneider et al., 2002; Seluchi et al., 2003). The south-westerly winds are characterised by different effects. Because of much lower mountain ranges and a fjord-like landscape, these winds lose less moisture and are able to increase their water load while passing for example the Strait of Magellan. Therefore, a certain precipitation supply in the catchment of Laguna Potrok Aike is due to these south-westerly winds. As Mayr et al. (2007a) have already shown, the highest absolute amount of precipitation (up to 150 mm) at Laguna Potrok Aike is related to this wind direction, while extreme rain events occur from easterly (up to 0.8 mm/h) and northern wind directions. These rare but heavy rains are due to a blocking situation of the SHW. Blocking situations occur statistically more often during an intensified meridional thermal gradient during the southern winter and a northward displacement of the polar and subtropical jets in the upper troposphere (Mendes et al., 2008). The persistence of the SHW throughout the year furthermore causes the dominance of zonal compared to meridional winds and the rareness of blocking action of the SHW.

As own observations during the last ten years showed, the amount of water in Laguna Potrok Aike is highly dependent on precipitation changes (Ohlendorf et al., 2013) but also strongly influenced by evaporation. In contrast to the relatively dry year from March 2001 to February 2002 with only 136 mm

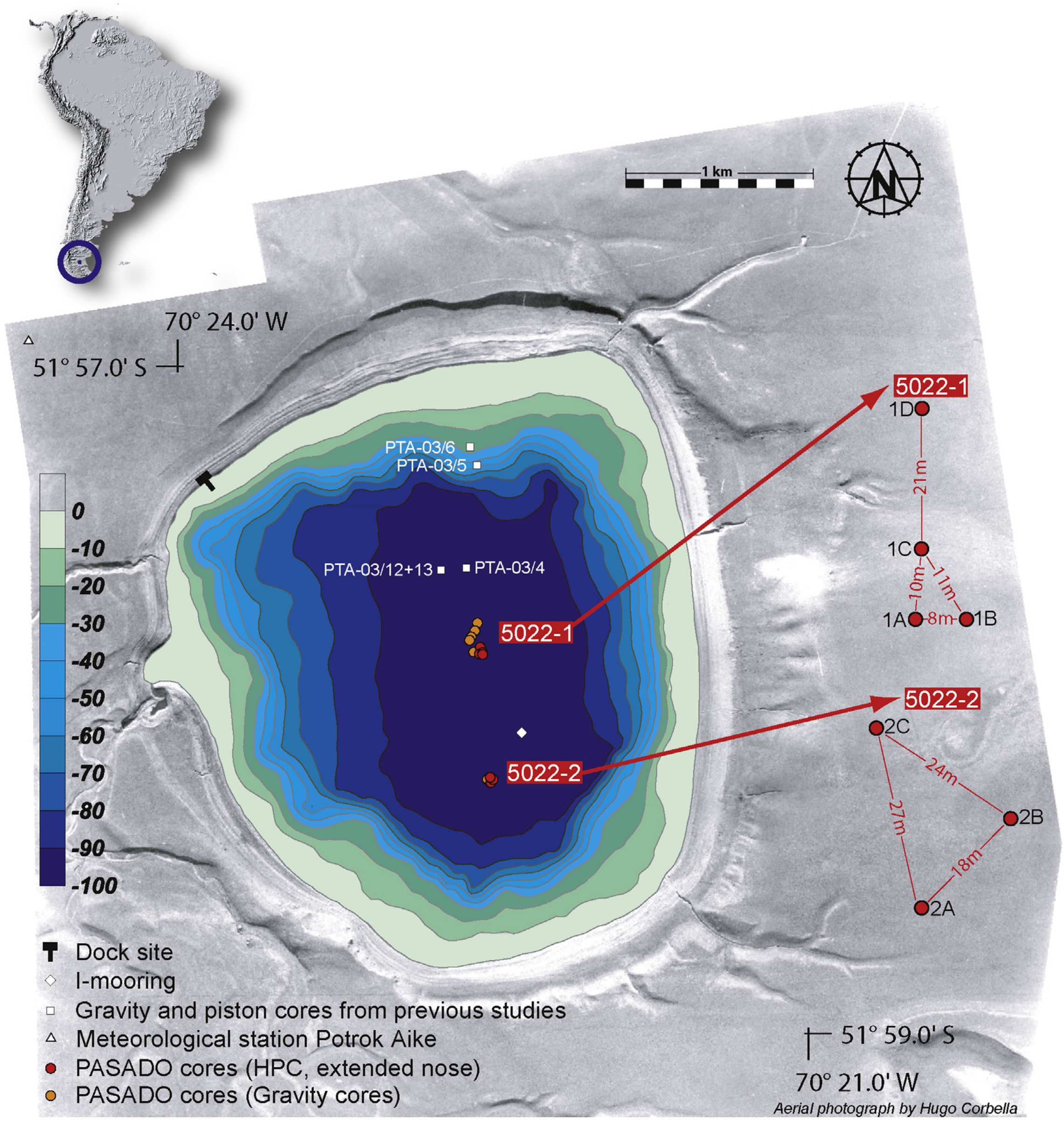

Fig. 1. Site location of Laguna Potrok Aike in southern Patagonia with bathymetry and the position of the drill cores (graphic by C. Ohlendorf).

precipitation, the lake level rose by ca 1 m during the following wet 12 months (Ohlendorf et al., 2013) which brought 270 mm of precipitation, while the yearly mean precipitation during the last 10 years is about 205 mm. Of course other climate factors like temperature, humidity and wind speed as well as the largely unknown groundwater influx also contribute to the amount of water that stays in the lake.

3. Material and methods

3.1. Pollen surface samples

101 pollen surface samples were collected during different field studies in southern Patagonia between 49°–54°S and 68°–73°W (Mancini, 1998, 2002; Prieto et al., 1998; Mancini et al., 2002). The orientation of sampling mainly follows the most important climatic gradient from east to west (Figs. 3 and 4), i.e., it forms three transects. The northernmost transect starts at the estuary of the Santa Cruz River at the Atlantic coast heading towards Lago Argentino, while the second transect stretches from Río Gallegos to Río Turbio and the southernmost transect is parallel to the Strait of Magellan from the east towards Punta Arenas. Because of the rareness of deep and constantly water-filled lakes in the Patagonian steppe region east of the Southern Andes, we took surface soil samples and analysed their pollen spectra as modern analogues. At each sampling location we collected the uppermost 1 cm of the soil surface at different positions within a 10 m^2 area representing a uniform vegetation type. Parts of the samples are included in the pollen surface samples data bank at Mar del Plata University, Argentina. The ecological and vegetational background related with these surface samples has been discussed in extenso by Quintana (2009).

3.2. Laguna Potrok Aike sediment core

Using a UWITEC piston-coring device, the 100 m deep maar lake Laguna Potrok Aike was cored in 2003 in the framework of the

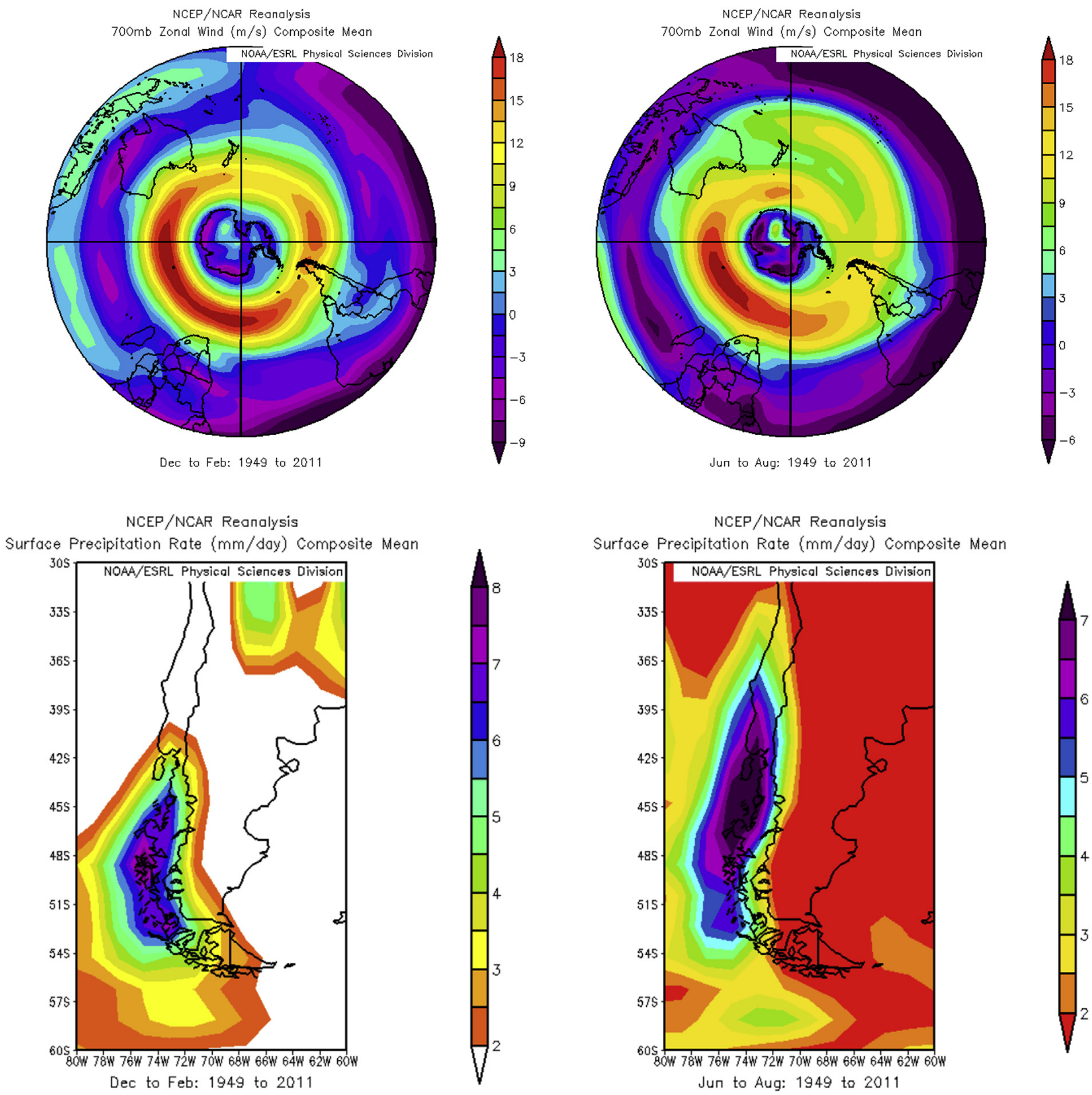

Fig. 2. Position of zonal wind and surface precipitation rate for southern summer and winter months. Data source: http://www.esrl.noaa.gov/psd/cgi-bin/data/getpage.pl; accessed 16.10.11, graphic by J.P. Francois.

SALSA project. Chronology of this nearly 20 m long core (a composite core of PTA02/4, PTA03/12 and PTA03/13, Fig. 1) dates back to 16 ka cal. BP (Haberzettl et al., 2007). For the age–depth model applied here see Kliem et al. (2013a).

3.3. Pollen analysis

Pollen samples from the Laguna Potrok Aike composite core were sampled every 4 cm, in key parts resolution was increased to 2 cm. Pollen sample preparation was carried out using standard techniques (HCl, KOH, acetolysis and ultrasonic sieving). Two tablets of *Lycopodium* spore marker tablets were added to each sediment sample before the treatments in order to calculate concentration values. For identification of the pollen grains our own reference collection was used accompanied by the pollen atlases of Heusser (1971) and Markgraf and D'Antoni (1978). Most of the 101 surface as well as the 241 fossil samples were counted to a minimum of 300–500 pollen grains. Only a few samples did not reach such a standard because of low pollen concentration. Pollen percentages were calculated based on the pollen sum of higher plants excluding aquatics (Wille et al., 2007).

3.4. Numerical analysis

Climate data were derived from the global database (Leemans and Cramer, 1991) and were attributed to each pollen surface sample by linear interpolation. The gradient of the yearly precipitation sum (P_{ann} in mm) is large and lies between 52 and 1055 mm. The mean annual temperature (T_{ann}) in the studied region is between 5.1 and 8.1 °C.

In order to understand the relationship between recent pollen taxa assemblages and climate we performed different statistical methods. First of all we reduced the data matrix of originally 57 taxa by including only the most important pollen-types reaching

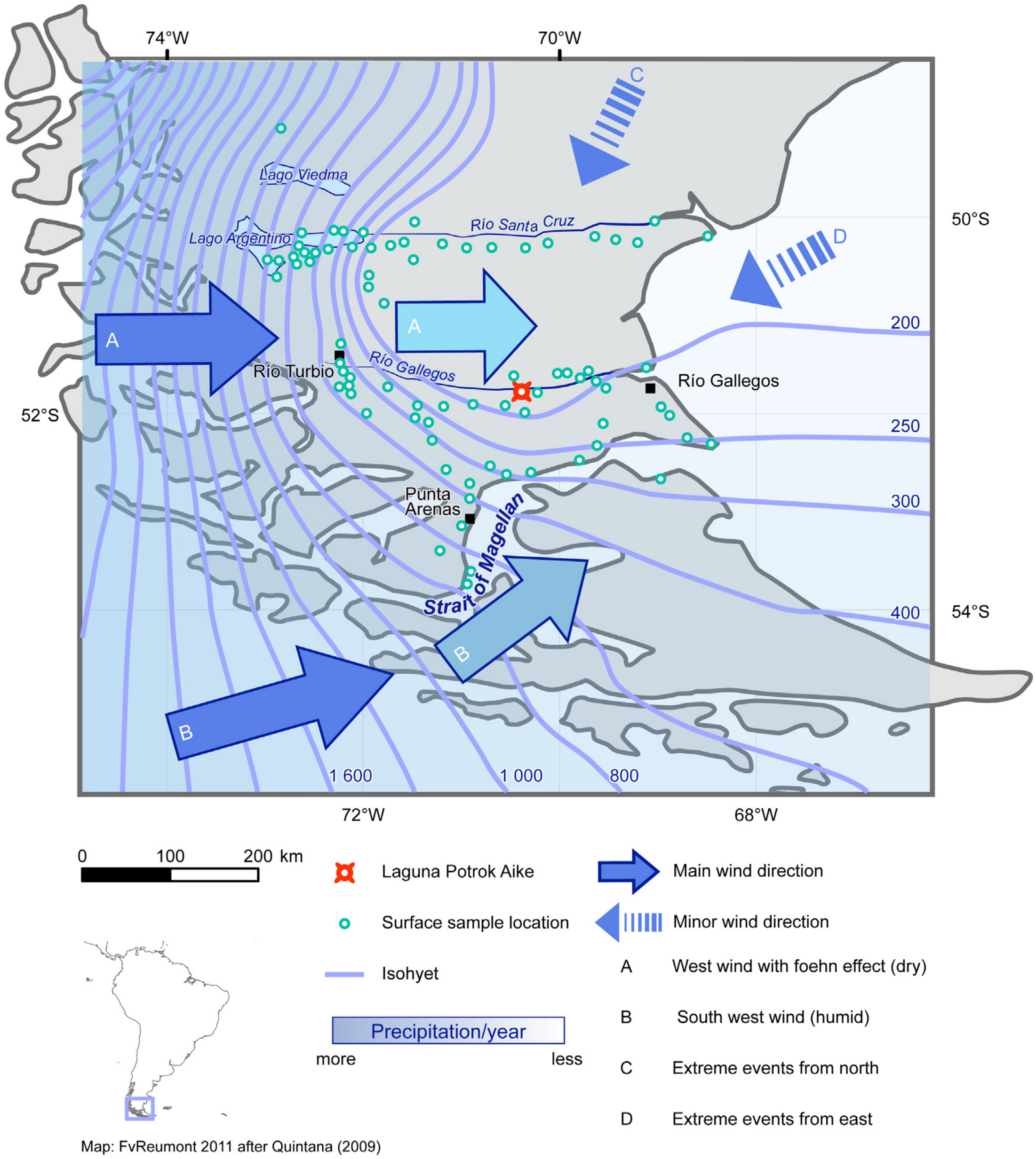

Fig. 3. Surface samples distribution, yearly precipitation and main precipitation sources in southern South America.

either more than 3% maximum once or appearance in at least more than 10% of all samples and reaching more than 2% maximum. Furthermore, we excluded the water plants (*Myriophyllum* and *Triglochin*) as well as *Rumex* and Polygonaceae because the last ones are strongly correlated to human impact (Heusser, 2003). With this procedure we reduced the amount of relevant taxa to 29 (Table 1). All further statistics were performed on this dataset.

Multivariate statistical methods for classification and ordination, such as unconstrained cluster analysis (Quintana, 2009) and Redundancy Analysis (RDA), were performed in order to reveal similarities among samples and relationship between pollen assemblage's climatic variables, respectively (Overpeck et al., 1985; Grimm, 1987; Xu et al., 2010; Legendre and Birks, 2012). Both analyses were performed on the recalculated percentages of the dataset ($n = 29$). Statistical correlations between the pollen surface dataset and selected climatic variables, yearly mean temperature (T_{ann}) and the yearly precipitation sum (P_{ann}), were calculated and tested utilizing RDA. For these procedures we logarithmically transformed the data in order to reduce the asymmetry of the distribution and normalized them by applying the interval scale transformation following Birks (2012). Detrended Correspondence Analysis (DCA) performed *a priori* indicates that gradient lengths are less than 2.3 standard deviations, suggesting that underlying responses are linear (Legendre and Birks, 2012). The pollen dataset was square-root transformed and treated with chord transformation, followed by calculation of the Euclidean distance (Legendre and Gallagher, 2001). Significance of the climatic variable was estimated performing unrestricted Montecarlo permutations ($n = 999$) afterwards to determine that collinearity among the explanatory variables was not significant (variance inflation factor < 10) (Table 2.).

For the development of the transfer function model we first used all the 101 soil surface samples and 29 pollen taxa (Table 1) and analysed them with the C2-programm routines (Juggins, 2003). A

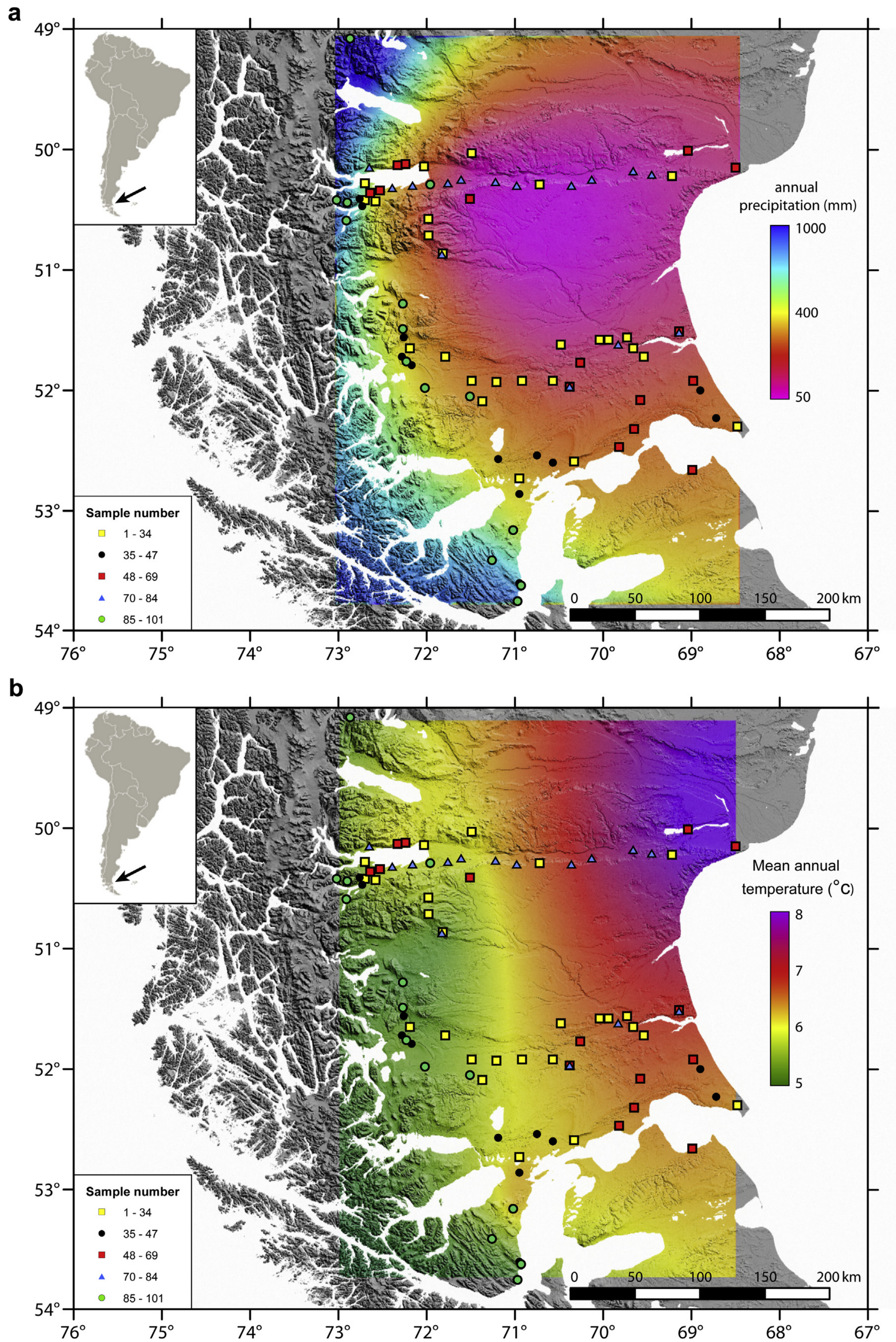

Fig. 4. Map showing the 101 surface samples and the two climatic variables used for the transfer function development. Colours of the samples refer to the main pollen groups in Fig. 5. a) Yearly amount of precipitation interpolated between the samples. b) Yearly mean temperature values interpolated between the samples. (For interpretation of the references to colour in this figure legend, the reader is referred to the web version of this article.)

Table 1
All 57 taxa in alphabetical order and their basic statistical values, the included 29 taxa for further analysis are marked in bold.

Nr.	Name	*N* non-zero values	Maximum	Mean	Standard deviation
1	***Acaena***	62	**14.12**	**1.27**	**2.34**
2	**Amaranthaceae/ Chenopodiaceae**	60	**46.08**	**1.35**	**5.82**
	Anacardiaceae	7	1.25	0.03	0.16
3	**Apiaceae**	70	**37.73**	**1.56**	**4.31**
	Araucariaceae	2	0.13	0.00	0.02
	Armeria	21	1.84	0.07	0.26
4	**Asteraceae subf# Asteroideae**	97	**40.74**	**7.81**	**9.28**
5	**Asteraceae subf# Cichorioideae**	73	**23.76**	**1.66**	**3.76**
6	***Berberis***	19	**14.05**	**0.22**	**1.41**
7	**Brassicaceae**	64	**14.71**	**1.57**	**2.90**
8	**Caryophyllaceae**	94	**26.01**	**3.21**	**4.05**
	Cupressaceae	4	0.42	0.01	0.05
9	**Cyperaceae**	92	**43.18**	**3.37**	**5.41**
10	***Drimys***	16	**2.89**	**0.06**	**0.32**
11	***Empetrum* type**	77	**52.18**	**3.93**	**8.71**
12	***Ephedra***	59	**44.13**	**2.64**	**5.99**
13	**Ericaceae type**	18	**18.23**	**0.53**	**2.36**
	Euphorbiaceae	20	1.78	0.09	0.28
14	**Fabaceae**	72	**24.12**	**1.18**	**2.80**
	Geraniaceae	26	1.48	0.11	0.30
15	**Gunnera**	30	**13.76**	**0.28**	**1.47**
16	**Lamiaceae**	35	**3.23**	**0.26**	**0.58**
	Liliaceae	1	0.14	0.00	0.01
	Malvaceae	19	1.87	0.13	0.39
	Maytenus	2	0.43	0.01	0.04
	Mimosaceae	1	0.20	0.00	0.02
17	***Misodendron***	28	**10.29**	**0.34**	**1.24**
18	**Monocotyledoneae**	14	**2.51**	**0.10**	**0.33**
19	***Mulinum***	28	**6.60**	**0.20**	**0.73**
	Mutisieae	3	2.53	0.03	0.25
	Myriophyllum	1	2.82	0.03	0.28
	Myrtaceae	4	0.16	0.00	0.02
20	***Nassauvia***	76	**32.92**	**2.46**	**5.15**
21	***Nothofagus dombeyi*-type**	100	**88.87**	**19.88**	**23.53**
	Nothofagus obliqua-type	8	2.75	0.05	0.29
	Onagraceae	3	0.16	0.00	0.02
	t# *Ovidia*	1	0.59	0.01	0.06
22	**Phacelia**	5	**7.08**	**0.09**	**0.71**
	Plantago	44	1.48	0.18	0.32
23	**Poaceae**	101	**82.94**	**38.12**	**21.00**
24	**Podocarpaceae**	69	**5.08**	**0.36**	**0.59**
	Polemoniaceae	2	0.31	0.00	0.04
	Polygala	6	2.03	0.03	0.21
	Polygonaceae	15	3.81	0.07	0.41
25	**Ranunculaceae**	23	**2.12**	**0.08**	**0.26**
	Rhamnaceae	1	0.14	0.00	0.01
26	**Rosaceae**	30	**7.41**	**0.44**	**1.13**
27	**Rubiaceae**	22	**6.15**	**0.17**	**0.68**
	Rumex	86	66.97	5.11	11.61
	t# Sapotaceae	1	0.17	0.00	0.02
	t# Saxifragaceae	1	0.35	0.00	0.03
28	**Solanaceae**	39	**6.09**	**0.34**	**0.84**
	Triglochin	12	14.14	0.22	1.45
	Tropaeolaceae	1	0.20	0.00	0.02
	Valerianaceae	17	0.67	0.05	0.13
29	**Verbenaceae**	25	**8.49**	**0.26**	**1.01**
	Violaceae	1	0.08	0.00	0.01

logarithmic transformation was performed on all pollen percentages before developing the transfer functions in order to stabilize the variance and to reduce the statistical noise. Different transfer function algorithms were tested (MAT = Modern Analogue Technique, WA = Weighted Average and WAPLS = Weighted Average Partial Least Square) in order to find the most appropriate calibration model in a leave-one-out cross-validation procedure. For the MAT the Squared Chord Distance (SCD) and the Squared-Chi-Squared (SCS) algorithms were used for estimating the climate variable including the 10 closest surface samples into the calculation. For determination of the statistically reliable components of each model, the performance data were compared (Table 3). The chosen model should show a high R^2 (coefficient of determination between predicted and observed climate values), low RMSEP (Root Mean Square Error of Prediction) and a low maximum bias. For the regression models the smallest number of useful components should be chosen. This is determined by a decrease of less than 2% towards the lower number of components (Birks, 1998). Furthermore, scatter plots between observed and predicted values document the statistical relevance of the chosen model. By that check, four outliers were identified in the precipitation and two in the temperature model. Thereupon, the calculations were repeated without these samples (only 97 for the precipitation model), which partially increased the performance of the models.

Table 2
Results of DCA and RDA analysis on 101 surface pollen samples and 29 pollen taxa for 2 climate variables in southern Patagonia.

Climatic variable	AX1	AX2	P_{ann}	*p*-value	Percentages of explained variance (total 25%)
P_{ann}	0.790	0.078	–	0.001	22%
T_{ann}	−0.619	0.340	−0.676	0.001	3%
Species–environment correlations	0.779	0.538	–		–

4. Results

4.1. Surface pollen data

Five main groups were identified by the help of unconstrained cluster analysis (Fig. 5), which follow a west-to-east regional distribution (Fig. 4a and b). The samples characterizing **Group 1** (grass steppe; Nr. 1–34, yellow) exhibit high amounts of pollen from Poaceae (max. 84%), Brassicaceae, Cichorideae and abundant Cyperaceae but not more than 22% of *Nothofagus dombeyi*-type pollen. They occur in regions with low yearly precipitation (mean 209 mm/a) but relatively high yearly mean temperatures (mean 6.1 °C). **Group 2** (forest steppe transition; Nr. 35–48, grey) is codominated of Poaceae (max. about 60%), and *N. dombeyi*-type (up to 50%), encompassing by *Empetrum rubrum* type and Asteroideae pollen. This assemblage coincides with an increase in rainfall (mean 360 mm/a) and slightly less yearly mean temperatures (mean 5.9 °C) than the grass steppe. **Group 3** (shrub steppe; Nr. 49–64, red) is characterized by relative high amounts of Poaceae (max. of 47%) and Asteroideae (max. 49%) pollen. Caryophyllaceae, Apiaceae, Rubiaceae, Solanaceae and Verbenaceae appear also like characteristic taxa. Whereas *N. dombeyi*-type pollen never reaches more than 15%. These assemblages occur in areas with relatively high yearly mean temperatures (mean 6.3 °C) but only low amounts (221 mm/a) of precipitation. In **Group 4** (dwarf-shrub steppe; Nr. 65–84, blue) pollen of Poaceae is dominant (max. up to 68%), and accompanied by high amounts of different shrubby taxa such as Asteroideae, *Ephedra*, *Nassauvia* and herbs like Caryophyllaceae and Chenopodiaceae/Amaranthaceae. *N. dombeyi*-type pollen never reaches more than 26%. Climatically this group is characterized by lowest amounts of yearly precipitation (mean 152 mm/a) but highest yearly temperatures (6.6 °C), except for the samples with high amounts of *Nassauvia*, retrieved from relative high altitude areas and characterizing cooler

Table 3
Performance of the reconstruction models. Model names: MAT = Modern analogue technique (average of the ten closest analogues), WMAT = Modern analogue technique (weighted average of the ten closest analogues) SCS = Squared Chi-squared Distance, SCHORD = Squared Chord Distance; WA = weighted averaging with -Inv = inverse deshrinking, -Cla = classical deshrinking; WAPLS = weighted averaging partial least squares regression, C1–C5 = Number of components included. Performance variables: R^2 = coefficient of determination between predicted and observed climate values, Max. bias = maximum bias (statistical noise), RMSEP = root mean square error of prediction, %Change = % decrease in RSMEP towards higher component number. In bold: the best model of each set of algorithms.

Annual precipitation (mm)					Annual mean temperature (°C)			
Model	R^2	Max. bias	RMSEP	%Change	R^2	Max. bias	RMSEP	%Change
Models with all 101 surface samples								
MAT SCS	0.7978	387.505	124.327		0.4230	1.2863	0.4994	
WMAT SCS	**0.8383**	**249.694**	**107.464**		**0.4562**	**1.2594**	**0.4851**	
MAT SCHORD	0.7897	401.74	128.017		0.4079	1.28074	0.5054	
WMAT SCHORD	0.7903	400.509	127.836		0.4082	1.2806	0.5053	
WA_Inv	**0.7605**	**250.994**	**120.197**		**0.4984**	**1.1324**	**0.4996**	
WA_Cla	0.7605	212.557	132.183		0.4984	0.5494	0.6805	
WATOL_Inv	0.7086	325.539	135.471		0.4415	1.3678	0.5288	
WATOL_Cla	0.7086	192.634	148.565		0.4415	0.689	0.7616	
WAPLS C 1	0.7605	245.027	119.797		0.4983	1.1021	0.5013	
WAPLS C 2	**0.8284**	**175.674**	**110.109**	8.0867	**0.6459**	**0.9355**	**0.4668**	6.8684
WAPLS C 3	0.8445	140.748	108.38	1.5706	0.6778	0.8568	0.4697	−0.6107
WAPLS C 4	0.8546	133.638	111.403	−2.789	0.6882	0.9038	0.4887	−4.0429
WAPLS C 5	0.8599	123.491	113.188	−1.603	0.6958	0.8232	0.5045	−3.2222
Models without four outliers for P_{ann}: 85, 86, 87, 89								
WAPLS C 1	0.7389	207.917	92.328					
WAPLS C 2	**0.7905**	**144.918**	**90.129**	2.38202				
WAPLS C 3	0.8100	135.406	92.6527	−2.7999				
WAPLS C 4	0.8209	139.107	97.6545	−5.39853				
WAPLS C 5	0.8238	147.271	99.9426	−2.34303				

conditions. **Group 5** (forest; Nr. 85–101, green) show the lowest amounts of Poaceae (max. 30%) but the highest values for *N. dombeyi*-type (max. 92%). Associated taxa are *E. rubrum* type pollen, *Gunnera* and *Misodendrum*. This group occurs in areas with the highest amounts of annual precipitation (mean 630 mm/a) and lowest yearly mean temperatures (5.5 °C). It is worth to mention, that *N. dombeyi*-type pollen not only occurs in the forest and forest-steppe ecotone, where this floristic element is growing, but also in the drier steppe environments denoting its long distant transport feature (Mancini, 1998; Schäbitz, 1999; Quintana, 2009). This is also true, but not as extreme, for other forest elements as *Drimys*, *Gunnera* and Podocarpaceae highlighting the strength and dominance of the prevailing west winds in the region.

4.2. Canonical ordination

According to the RDA 25% of the total pollen variance is explained by the climatic variables P_{ann} and T_{ann} (Table 2). Unrestricted Monte Carlo permutations prove the significance (p-value < 0.001) of both climatic variables. Results indicate that both variables are strongly correlated with axis 1 ($\lambda = 0.227$) which captures more than 90% of the explained variance. The P_{ann} variable exhibits a positively correlation with axis 1 ($r = 0.79$) whereas T_{ann} shows a negative correlation ($r = -0.62$) with it (Table 2). The species and climatic variables show also a strong correlation with axis 1 ($r = 0.80$), a weaker correlation with axis 2 ($r = 0.54$). The inter-correlation between the environmental variables is negative ($r = -0.68$).

The biplot (Fig. 6: colours (in the web version) of samples correspond to the ones used in Fig. 5) shows how the samples from the groups 2 and 5 are positioned in the right side of the biplot, together with species such as *Nothofagus*, *Misodendron*, *Drimys*, *Empetrum*, and Ericaceae, and denoting a positive (negative) correlation with the variable P_{ann} (T_{ann}). On the other hand, samples from group 4 are located in the left side, together with taxa such as Poaceae, *Nassauvia*, Asteraceae, Caryophyllaceae, *Ephedra*, Amaranthaceae, Verbenaceae and others, and denoting an opposite trend to the observed in the groups 2 and 5. While samples from the groups 1 and 3 are located in the middle of the biplot suggesting the interplay of both climatic variables. In Fig. 6A four samples are identified (Nr. 85, 86, 87 and 89) representing the northernmost locations and with exhibiting higher *Empetrum* values. These are the same samples, which were determined as outliers during the development of the transfer functions.

4.3. Pollen climate calibration

As shown in Table 3 the WMAT-SCS, the WA-Inv and the WAPLS algorithms with two components reach good statistical performances mainly for P_{ann} and to a much lesser extend to T_{ann} on the base of 101 soil surface samples. Comparing all three methods for the best estimate of precipitation, WA-Inv shows the lowest performance ($R^2 = 0.76$, max. bias 250 mm and RMSEP 120 mm) and was excluded from further application. The remaining two methods have nearly similar R^2 (0.84 with WMAT SCS and 0.83 with WAPLS-C2) and RMSEP values (107 mm for MAT SCS and 110 mm for WAPLS-C2). But the maximum bias is considerable lower in the WAPLS-C2 approach: 175 versus 249 mm for MAT-SCS. Comparing the models for the annual temperature estimations, the validity of the WAPLS-C2 algorithm is visible ($R^2 = 0.64$, RMSEP = 0.47 and max. bias = 0.90), but the performance is much worse than for the estimation of precipitation. Because of these statistical uncertainties involved, temperature estimates will not be discussed and further used.

Finally, the elimination of the identified four outliers (see above) improved the performance of the WAPLS models during the second run of model construction for the calibration of precipitation. With a slightly smaller R^2 (0.79) as before but a considerably lower RMSEP (90 mm) and lowest maximum bias (144 mm) this model was chosen for further use. In Fig. 7 the scatter plot of the predicted precipitation values versus the observations (left panel) illustrates the statistical robustness of our model while the residuals versus the observations (right panel) demonstrate that our precipitation model overestimates lower precipitation values (range between 50 and

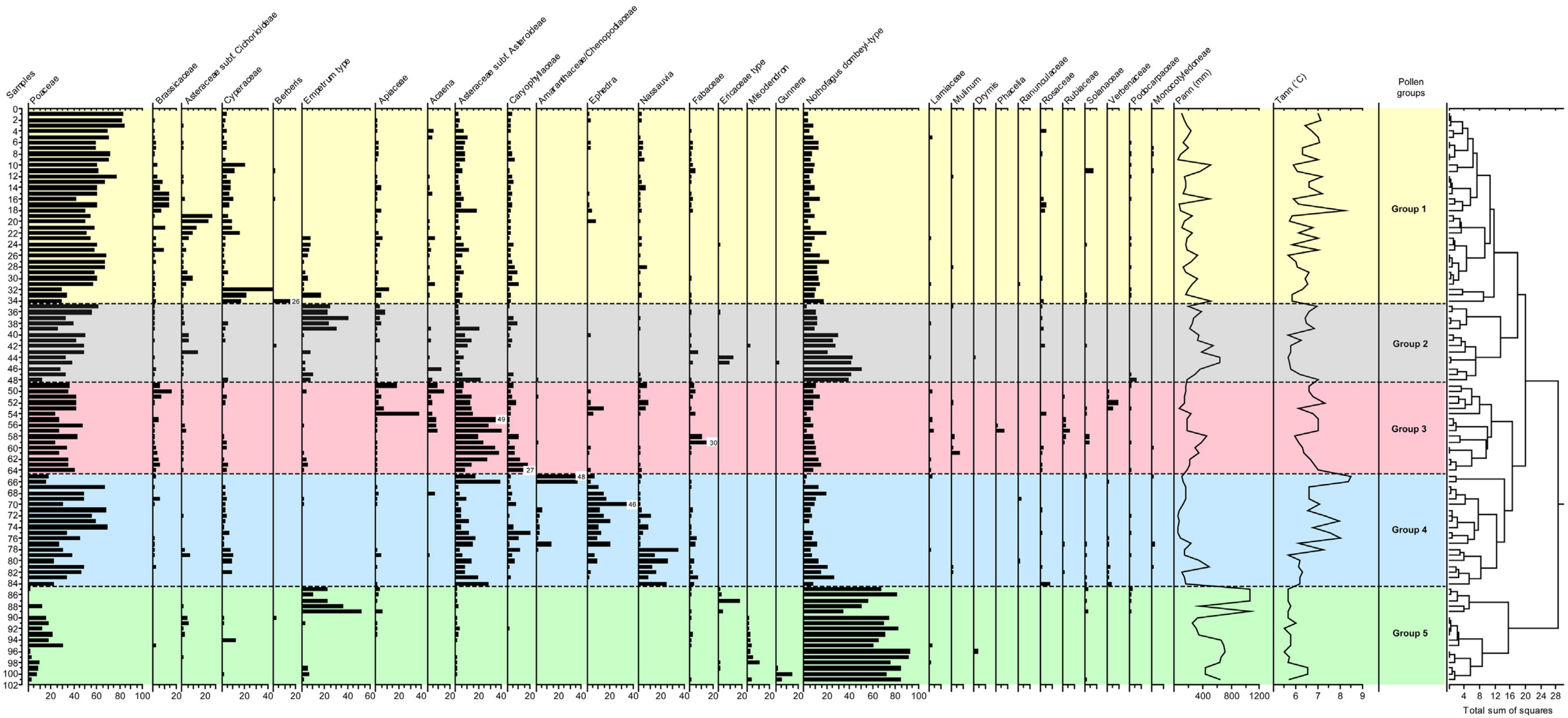

Fig. 5. Relative pollen diagram of the 101 surface samples and the 29 pollen taxa ordered by cluster analysis. Numbers of the samples and colours used for the main pollen groups refer to Fig. 4. Added are the precipitation (P_{ann}) and temperature (T_{ann}) data used for each sample. (For interpretation of the references to colour in this figure legend, the reader is referred to the web version of this article.)

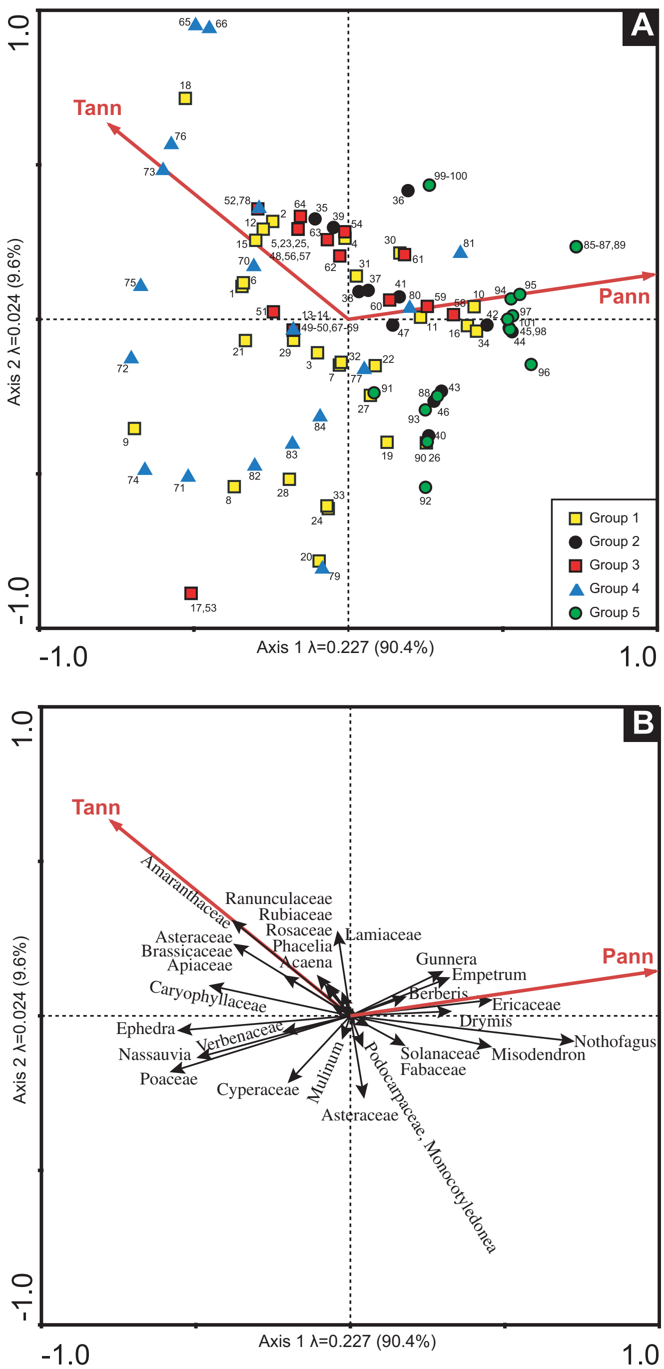

Fig. 6. Biplot showing the first two axes of the RDA ordination for the modern surface samples (A) and taxa (B) versus significant climatic variables. Correlation and probability values are shown in Table 2.

300 mm/year) whereas it underestimates in the higher range (>300 mm/year).

4.4. Quantitative climate reconstruction for Laguna Potrok Aike

Based on the presented WAPLS transfer function model palaeoprecipitation values are estimated for the Laguna Potrok Aike sediment record reaching back to 16 ka cal. BP (Fig. 8d). The estimated precipitation ranges between 424 (2017 cal. BP) and 158 mm (199 cal. BP) with a Holocene mean of about 276 mm and a Lateglacial mean of 249 mm. It should be kept in mind that for this range the model generally overestimates the precipitation amounts; therefore, the real amounts would have been probably lower than predicted. In the following we will discuss the trend line in Fig. 8d calculated by the C2-software using the lowest smooth (span: 0.05; 10 iterations) algorithm (Juggins, 2003). Shown by the trend line, precipitation was first slightly increasing between 16 and 14.8 ka cal. BP and then decreasing (from 270 to 235 mm) until around 12.2 ka cal. BP. Afterwards the trend smoothly increased for about 500 years before falling back to less than 240 mm until 11 ka cal. BP. Towards the Early Holocene (until around 9.6 ka cal. BP) the estimated precipitation amounts continuously rise to about 280 mm and then smoothly decrease until 9.3 ka cal. BP. The trend then increased to about 290 mm followed by a decrease down to 220 mm until 8.2 ka BP when an increase to 280 mm during the next 400 years follows. Starting at 7.8 ka cal. BP the trend line decreases again to 240 mm and first remains low while later decreases to 235 mm/a until 6.3 ka cal. BP. Afterwards rising and slightly higher precipitation values (290 mm) are visible until 5.5 ka cal. BP, followed by lower amounts of about 240 mm until 4 ka cal. BP. From this time on the values continuously rise until today (up to 360 mm), reaching a peak around 2 ka cal. BP (320 mm) but showing smaller amounts around 1.3 ka cal. BP (275 mm) and 300 years ago (300 mm).

5. Discussion

The cluster analysis performed on the base of pollen surface samples, shows a close relation to the main and most important vegetational units occurring in southern Patagonia (Fig. 5), feature that also have been identified in other studies (i.e., Mancini, 1993, 1998; Prieto et al., 1998). The canonical analysis (RDA) denotes the interplay of the climatic variables P_{ann} and T_{ann} in the pollen variation along the studied area. Nevertheless our transfer function modelling shows that the WAPLS algorithm predicts P_{ann} much better than T_{ann}. We interpret this result due to a very low temperature gradient (5.1–8.1 °C), compared to the dominant precipitation gradient (52–1055 mm or 52–706 finally used in the reconstruction with 97 samples) occurring along the region. On the other hand the tested climatic variables explain only about one third of the pollen variance, suggesting other underlying mechanisms controlling the pollen, and hence vegetational variation. Possible factors influencing the vegetation must be related with features controlling the available water content for the plants (i.e., evapotranspiration and grain-size composition of the soils), which strongly influence the ecology of the plant communities especially in semi-desert regions like Patagonia (i.e., Boelcke et al., 1985). Comparing the performance of our precipitation model – especially the RMSEP% and maximum bias% in relation to the precipitation range of the studied region – with published pollen precipitation calibrations (Seppä et al., 2004; Herzschuh et al., 2009) our model shows reliable values (Table 4).

The close modern correlation between precipitation and water levels for Laguna Potrok Aike (Ohlendorf et al., 2013) and the fact, that key modern pollen assemblages respond to the precipitation gradient in southern Patagonia strongly supports the use of transfer functions based on pollen data. The presence of these key modern pollen assemblages in the fossil record may allow to reconstruct the palaeoprecipitation amounts and compare them with former lake level changes. But due to its theoretical setting the results of precipitation transfer functions should be discussed with caution. The model construction is based on a spatial comparison of recent climate–vegetation–pollen relationships, but the model is used for a quantitative palaeoclimate reconstruction back in time (i.e., Birks, 1998; Birks et al., 2010). Generally spoken, the relationship between climate and pollen rain may vary during the investigated

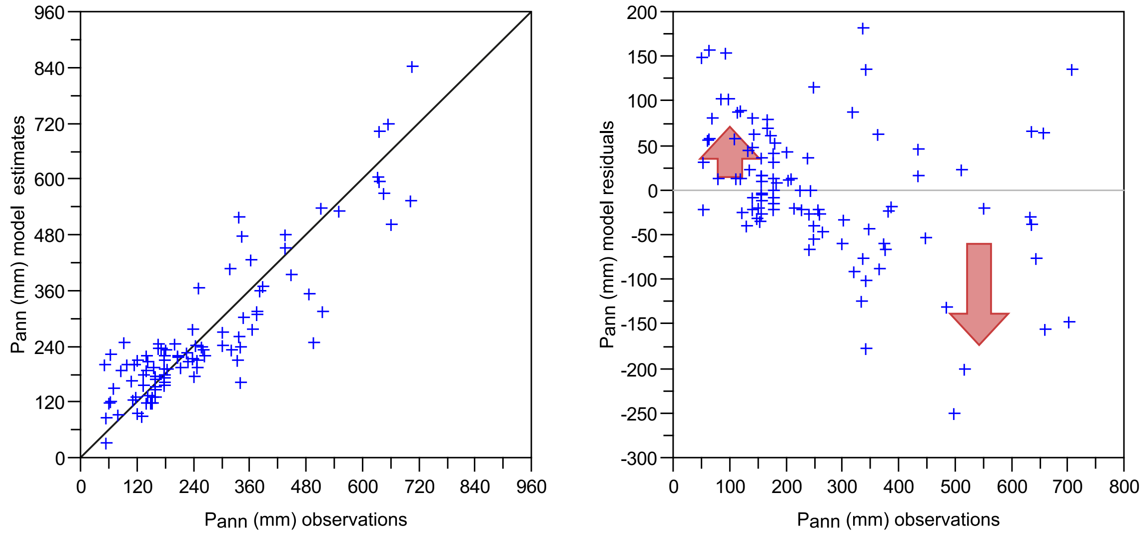

Fig. 7. Scatter plots of WA-PLS estimates (left) and residuals (right) of the precipitation model versus observed annual precipitation (P_{ann}).

time interval. In our case, especially during cold Glacial and Late-glacial times, when frozen ground played a major role in southern South America the environmental setting was different compared with recent times. Nevertheless, the main pollen taxa identified as key variables for the climate reconstruction in our RDA occur throughout the profile of Laguna Potrok Aike, only their amount is changing through time. Therefore, the use of the prediction model should give reliable results within the shown limitations. The model estimates mean annual precipitation values, which are a mix of different air humidity sources transported to Laguna Potrok Aike, and cannot be differentiated. Changing wind directions trigger different pathways for humid air reaching Laguna Potrok Aike. To evaluate the reliability and strength of our palaeoprecipitation estimates, data will be (a) compared with other proxies from Laguna Potrok Aike and (b) discussed in a regional context.

5.1. Comparison with other proxies from Laguna Potrok Aike

For internal comparison we chose the Ca/Ti ratio (Haberzettl et al., 2009) as a complementary data to interpret hydrological variability in the Laguna Potrok Aike record (Fig. 8c). High values in the Ca/Ti ratio occur during drier phases, whereas low values responding to times of increased moisture availability (Haberzettl et al., 2009). These results highlight at least four pronounced dry phases: 1) during the Mid-Holocene climate optimum (8.7–7.2 ka cal. BP) with two very pronounced peaks around 8.2 and 7.5 ka cal. BP, 2) between 4.6 and 3.8 ka cal. BP, 3) during the Medieval Climate Anomaly (MCA, 1.3–0.5 ka cal. BP) and 4) during the 20th Century Warming (Fig. 8c). These dry phases were also discussed based upon pollen and diatom assemblages by Wille et al. (2007). There is a partial but not complete agreement between these dry periods and our precipitation estimates for the Holocene. The late Early- and Mid-Holocene periods (8.2; 4.6–3.8 ka cal. BP) are clearly mirrored by lower precipitation estimates reconstructed by our model. Moreover, Wille et al. (2007) mentioned the abundance of the diatom *Cyclotella agassizensis* between 8.5 and 8.0 cal. BP indicative for low lake levels. Also the second remarkable dry spell around 7.5 ka cal. BP recorded in the Ca/Ti ratio by Haberzettl et al. (2009) is indicated in our data, as precipitation decreased from 7.8 ka cal. onwards and remains on lower values until 7.0 ka cal. BP. Another dry Holocene period in our model is the time around 4 ka cal. BP, which coincides well with the geochemical indicators used by Haberzettl et al. (2009).

The MCA is characterized by fluctuating precipitation amounts in our reconstruction, first low, then rising. The 20th century warming shows the opposite trend with an increase in precipitation estimates while lake levels are lower. In the overall trend, the driest time of the Holocene between 8 and 2.5 ka cal. BP with the highest Ca/Ti ratio also shows the lowest precipitation values, which were generally lower than the Holocene mean calculated from our data.

Compared with the palaeoshoreline reconstruction of Anselmetti et al. (2009), who reconstruct rising lake levels of Laguna Potrok Aike by identifying palaeoshorelines in seismic investigations based on interpolated radiocarbon ages, our modelled precipitation data only show partial agreement (Fig. 8b). Anselmetti et al. (2009) proposed a general rise of lake levels between 6.8 and 6 ka cal. BP, after 5.5 until 4.8 ka cal. BP, around 3.5 ka cal. BP and mentioned the Little Ice Age high stand already detected by Haberzettl et al. (2005). Our precipitation model shows first stable then decreasing values for the time interval between 6.8 and 6.2 ka cal. BP, followed by an increase until 5.5 ka cal. BP. Thereafter, modelled precipitation decreases until 4 ka cal. BP showing rather stable values between 4.9 and 4.5 cal. BP. Later on the precipitation estimates are in accordance to the general rise of lake levels at Laguna Potrok Aike including the lake level high stand at the end of the LIA.

The reasons for the discrepancies between both proxies are complex. Differences between them may first be related to the fact that the ages of seismically detected shorelines results from age interpolations of the original ^{14}C measurements between neighbouring palaeolake levels. Second, higher lake levels result from different direct and indirect climatic forcing factors, in which as discussed by Ohlendorf et al. (2013) – due to intensive winds and/or higher temperatures – evaporation and groundwater play a major role.

Generally, a warmer climate leads to a higher absolute amount of humidity in the air. This could at least be the reason for generally higher precipitation values in our model during the Holocene compared to the Lateglacial. Furthermore, higher temperatures in combination with high wind speeds can lead to a rise in the amount of evaporation. Therefore, even higher precipitation during the Holocene will not result in a higher lake level of Laguna Potrok Aike as long as this surplus in the amount of water is overcompensated by higher evaporation. This could especially have been the case during Mid-Holocene warmer phases (around 8 ka), when our

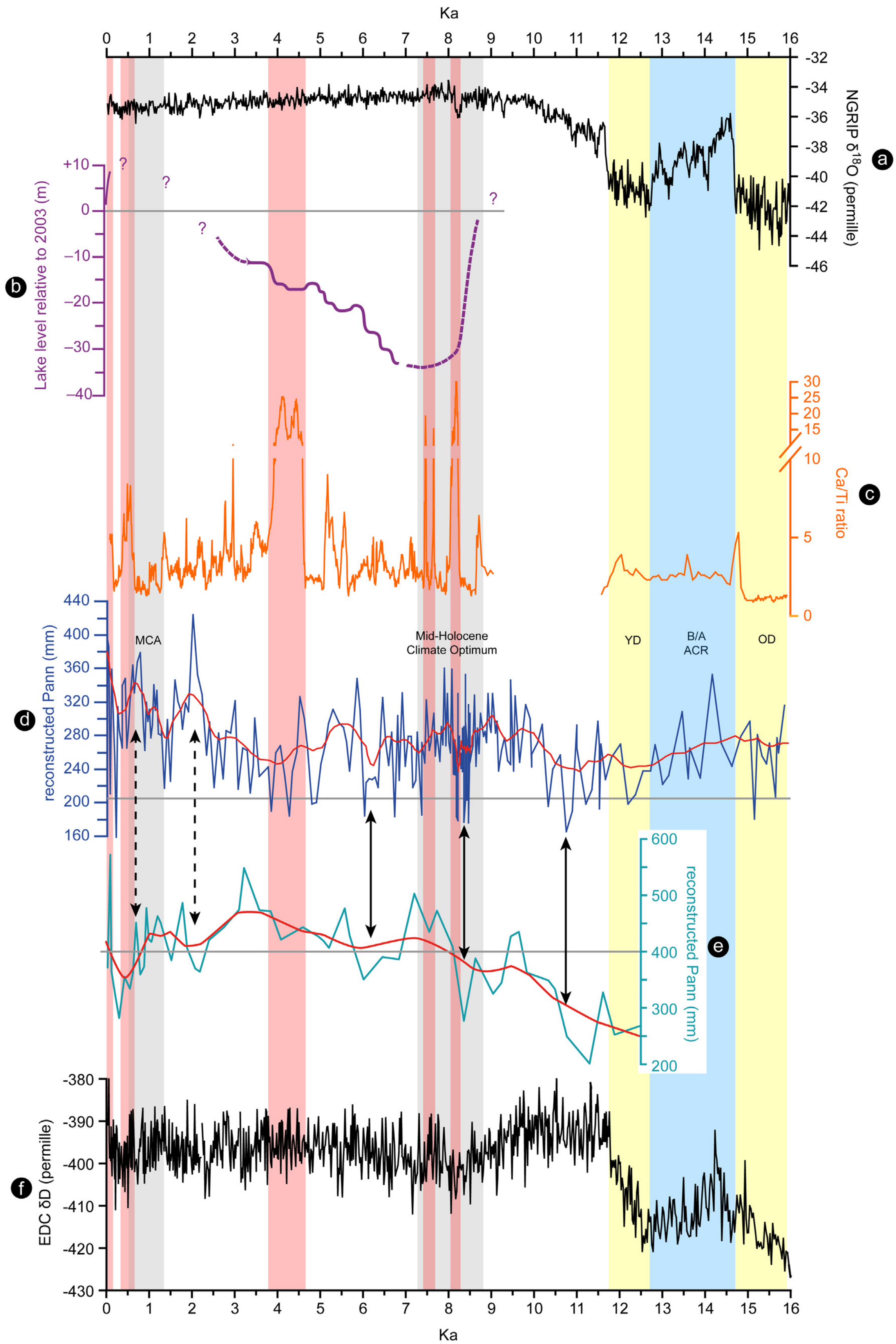

Fig. 8. Reconstructed palaeoprecipitation at Laguna Potrok Aike (d) compared with other selected proxies utilized to reconstruct the hydrological variability in the basin: The (b) palaeoshoreline reconstruction (based on Anselmetti et al., 2009), and (c) Ca/Ti ratio (Haberzettl et al., 2009). In addition we show the isotope record from (a) North Greenland (NGRIP-Members, 2004) and (f) Antarctic (EDC; Jouzel et al., 2007), and (e) the palaeoprecipitation record for Cerro Frias (based on Tonello et al., 2009). The red line denotes the

Table 4
Performance comparison for P_{ann} (mm). For names and performance abbreviations compare Table 1. RMSEP% = root mean square error of prediction in relation to the precipitation range of the studied region, Max. bias for range = Maximum bias (statistical noise) in relation to the precipitation range of the studied region.

Name	RMSEP (mm)	R^2	Max. bias (mm)	Area/no. of samples	Range (mm)	RMSEP%/max. bias for range	Author
WAPLS-C2	90	0.79	144	South Patag./97	52–706	13.7/21.9	This study
WAPLS-C1	104	0.75	205	Tibetan Plat./112	31–1022	10.5/20.7	Herzschuh et al., 2009
WA-PLS-C2	58	0.77	80	Finland	395–717	18.0/24.8	Birks and Seppä, 2004

model shows increasing rainfall while there was no evidence for higher lake levels. Moreover, under a more pronounced seasonal climatic differentiation with more rain or snow during winter times but warmer and perhaps windier summer conditions, the net water balance of the lake could have become negative. Other authors discuss that stronger regional seasonality gives hints for such a scenario during Mid-Holocene times (Markgraf, 1993; Wagner et al., 2007; Wille et al., 2007). Of course, the resolution of the sediment core samples presented here does not allow annual or even seasonal differentiation, but such short-term changes and their influence on lake level fluctuations should generally be taken into account. Stronger winds and therefore higher evaporation are mainly related to SHW storm tracks: when they (i) are centred in more southern latitudes and/or (ii) become more intense due to a higher pressure gradient between cold Antarctic and warm subtropical air masses (Lamy et al., 2010). This led to the hypothesis that it might be possible to detect phases with higher west wind intensity in our Holocene data not only by high amounts of Andean forest taxa (Mayr et al., 2007a) but also whenever the combination of higher precipitation with a lower lake level occurs. If, in contrast, higher precipitation and higher lake levels occur together, this may be indicative for a more frequent easterly wind influence at Laguna Potrok Aike.

Other authors discussed the variations in SHW intensity on the base of a comparison between pollen and charcoal data from north- and southwest Patagonia, which indicates low but increasing SHW intensity for southern Patagonia between 13 and 10.5 ka BP, decreased intensity between 10.5 and 7.8 and “a sustained increase afterwards” (Moreno et al., 2010), which is in accordance with our reconstruction for Early- and Mid-Holocene times. Even for the Late Holocene and despite the general increasing trend, a weakening of the SHW is visible between 4 and 2.8 ka and around 0.5 ka in the data of Moreno et al. (2010, Fig. 2) and supports our interpretation.

Regarding the Lateglacial, there was no calcite precipitation in Laguna Potrok Aike for most of the time due to a higher lake level (Haberzettl et al., 2009; Ohlendorf et al., 2013). OSL-dated lake sediments exposed at the uppermost terrace level imply a very high lake level at 17 ka cal. BP at Laguna Potrok Aike (Kliem et al., 2013b). These supposed higher lake levels for the Lateglacial, are in contrast to the generally low precipitation inferred from the pollen based transfer model. This high lake level persisted until 8.3 ka cal. BP with probably one exception: the time period between 13.4 and 11.6 ka cal. BP which temporally compares to the Younger Dryas of the Northern Hemisphere (Haberzettl et al., 2007; Hahn et al., 2013). This contradiction to our precipitation reconstruction can be explained assuming that the lake level during Lateglacial times is mainly controlled by increased surface runoff from the catchment area related to the prevailing permafrost conditions. Combined with a reduced amount of evaporation under colder climate conditions additionally suppressed by longer ice cover during winter and a hampered groundwater loss due to a deep permafrost this can induce high lake levels with less annual precipitation (Ohlendorf et al., 2013). The latter stated that climatic changes in the range of only 15–17% within 60 years are sufficient to produce lake level fluctuations at Laguna Potrok Aike between −33 and +22 m (relative to the 2003 lake level). Compared to the Lateglacial mean of 249 mm the predicted palaeoprecipitation amounts for the Lateglacial they fluctuate considerably and sometimes more than these 15–17%.

5.2. Regional comparison

Interesting findings surge from the comparison between our reconstructed palaeoprecipitation and isotopic records from polar ice cores (Antarctica and Greenland, Fig. 8f and a). We observe a slight increase of the estimated precipitation between 16 and 14.8 ka cal. BP which correlates to the slow but continuing warming in Antarctica and the cooling in Greenland (Oldest Dryas) (Pedro et al., 2011). Later, during the Antarctic Cold Reversal (ACR) and the Bølling–Allerød (B/A), a decreasing trend of precipitation is appreciable, whereas towards the end of the following Younger Dryas (YD) with rising temperatures in Antarctic ice core records, our data indicates an increase of rainfall. These facts indicate – with a certain delay – an apparent positive (negative) correlation between Antarctic (Greenland) ice core data, denoting (i) an Antarctic signature in the SHW dynamic during the Lateglacial or (ii) a local hydrological response. The delay is may be due to the fact that the vegetational responses of climate changes always develop with a time lag.

Geomorphological studies indicate that during the ACR time glaciers appeared in the fjords of the Andes (Kilian et al., 2006), the Andean Mountains itself and the Strait of Magellan southwest of Laguna Potrok Aike was partly ice-covered (Mc Culloch et al., 2000; Kaplan et al., 2008a, 2008b) – latest around 15.3 to 12.3 ka cal. BP – which led to much drier air masses. During such conditions less precipitation has reached Laguna Potrok Aike by westerly or southwesterly winds, which is in good accordance with our model. Moreover, the colder climatic conditions occurring in the region during the ACR probably reduced the evaporation in the lake, resulting in a positive hydrological balance. This inference is partially supported by the fact that carbonate precipitation increases during the later period (YD) in the sediments of Laguna Potrok Aike, suggesting an increase in the evaporation in response to milder climate conditions (Haberzettl et al., 2007; Hahn et al., 2013). In other words, the hydrological changes registered during the Lateglacial in the Laguna Potrok Aike are strongly affected by the temperature, obscuring the precipitation signal.

smoothed trend in the reconstructed palaeoprecipitation of Laguna Potrok Aike and Cerro Frias, whereas the grey horizontal lines indicate the recent mean precipitation of 205 mm at (d) Laguna Potrok Aike and 400 mm at (e) Cerro Frias. Grey bars indicate well-known periods of hydrological change occurring in Patagonia (e.g. Mid-Holocene Climatic Optimum and Medieval Climate Anomaly). Red bars denote dry phases identified by Haberzettl et al. (2009). Yellow bars indicate the Younger Dryas (YD) and Oldest Dryas (OD), while the blue bar indicates the Antarctic Cold reversal (ACR) and the Bølling–Allerød (B/A). The arrows indicate events with analogous (continuous line) and opposite (dash line) trends between Potrok Aike and Cerro Frias precipitation reconstructions. See the text for details.

During the Holocene, terrestrial archives located in the vicinity of Laguna Potrok Aike which address the question about the SHW dynamic during the Post-Glacial, show different trends (Markgraf, 1993; Markgraf et al., 2003; Gilli et al., 2005; Villa-Martínez and Moreno, 2007; Mancini et al., 2008; Mancini, 2009; Tonello et al., 2009; Wille and Schäbitz, 2009; Markgraf and Huber, 2010; Moreno et al., 2010). This fact, already pointed out by Markgraf and Huber (2010), is probably the result by comparing different types of archives using different methods. Nevertheless, Kilian and Lamy (2012) suggest also that such phenomenon is related with our poor understanding about (i) the relation between precipitation and SWW strength at regional to local scale, (ii) the role of the evapotranspiration and temperature-related effect in the water balance, (iii) the edaphic features controlling the available moisture in soils, and (iv) the lack of high quality time control and temporal resolution in the records.

Despite these problems and limitations, the comparison of our data with the up today unique quantitative precipitation reconstruction for Southernmost Patagonia (Cerro Frias; Tonello et al., 2009) point out an interesting palaeoclimatic puzzle. We observe similar trends in both records during the first half of the Holocene, with remarkable dry phases around 11, 8.2, and 6.2 ka (Fig. 8d and e). Nevertheless, later during the second half of the Holocene, the records exhibit an opposite trend, with evident opposite patterns around 2 and 0.5 ka (Fig. 8d and e). The mechanism to explain this discrepancy is not clear. However, we observe that pollen records located towards the north of 50°S (e.g. La Tercera; Bamonte and Mancini, 2011) exhibit the same trend of decrease in the moisture availability during the last 3000 years like Cerro Frias, whereas pollen records located to the south of 50°S (e.g. Lago Guanaco; Moreno et al., 2010) indicate an increase in the moisture availability during this period. This pattern could indicate the proposed changes in the zonally symmetry/asymmetry experimented by the SHW dynamic during the Post-Glacial (Fletcher and Moreno, 2012). Nevertheless it is necessary to examine more in detail these palaeoclimatic inferences, in order to discard the role of other mechanisms not directly related with climate. For example, the role of the Andean topography, which changes abruptly around the latitude 50°S exhibiting higher (lower) altitudes to the north (south), a fact that probably modifies the relation between: wind strength, moisture transport, and evaporation.

5.3. Precipitation sources

As already pointed out the strength and position of the SHW seems to be the main factor for the precipitation supply west and east of the Andes (Schneider et al., 2002; Mayr et al., 2007b). But the west wind also may increase evaporation rates which in turn changes the net water balance of Laguna Potrok Aike to negative values and thus to lower lake levels. A moderate south-westerly wind on the other hand could have led to a sufficient base supply of moisture during the Holocene combined with less wind driven evaporation, which would increase lake levels at Laguna Potrok Aike without any stronger easterly influence. Therefore, the detailed picture of precipitation sources and the reasons for periods of drought in Southern Patagonia is more complicated than might be assumed and all aspects mentioned need to be considered in order to understand the past changes in the regional water cycle.

6. Conclusions

Our quantitative precipitation reconstruction based on pollen and climate data of southern South America is based on a statistically robust model. It overestimates lower and underestimates higher precipitation amounts, but works quite well in the range of rainfall typical for south-eastern Patagonian dry lands. It shows lower precipitation estimates for the colder Lateglacial than for the Holocene. During the Lateglacial the precipitation development seems to be closer related to temperature fluctuations known from Antarctic ice cores while during the Holocene it can be correlated to the influences of the SHW across the southern South American continent. Wind direction and wind strength strongly trigger the net water balance of Laguna Potrok Aike with three different scenarios: a strong west/southwest wind may result in a negative while a moderate west/southwest wind may result in a positive water balance of Laguna Potrok Aike as well as during easterly wind dominated events. Comparison of estimated precipitation values to Holocene lake level proxies and related palaeoshoreline development show some similarities but are not in complete accordance due to other environmental control mechanisms (evaporation, groundwater in- and out-flow) which are still not well known in their expression. Moreover, the pollen data reflect a regional climate signal, which may differ from the lake internal proxies. Nevertheless, the model is a reliable statistical tool for reconstructing the general trends of precipitation changes visible on longer time scales and potentially can be applied to full Glacial time intervals using the PASADO (Potrok Aike Maar Lake Sediment Archive Drilling Project) cores.

Acknowledgements

The authors thank all SALSA and PASADO research team members for their help with fieldwork and input during discussions. Moreover, we are thankful for getting the permission to use samples from Dr. A. Prieto of the recent pollen database located in the Laboratory of Palynology at the National University of Mar del Plata, Argentina. Furthermore, we thank the student helpers (Jonathan Hense, Catharina Casimir, Jan Wowerek) at the University of Cologne for their help during preparation of pollen samples. This research is a contribution to the German Climate Research Program DEKLIM (01 LD 0034 and 0035) where funds were obtained for the "South Argentinean Lake Sediment Archives and modelling" (SALSA) project. We would like to thank all these funding agencies for their financial support.

References

Anselmetti, F.S., Ariztegui, D., De Batist, M., Gebhardt, C., Haberzettl, T., Niessen, F., Ohlendorf, C., Zolitschka, B., 2009. Environmental history of southern Patagonia unravelled by the seismic stratigraphy of Laguna Potrok Aike. Sedimentology 56, 873–892.

Auer, V., 1946. The Pleistocene and Post-glacial Period in Fuego-Patagonia. In: Publ. Inst. Geogr. Uni. Hels., No. 12.

Bamonte, F.P., Mancini, M.V., 2011. Palaeoenvironmental changes since Pleistocene–Holocene transition: pollen analysis from a wetland in southwestern Patagonia (Argentina). Review of Palaeobotany and Palynology 165 (1–2), 103–110.

Birks, H.J.B., Seppä, H., 2004. Pollen-based reconstructions of late-Quaternary climate in Europe – progress, problems, and pitfalls. Acta Palaeobotanica 44, 317–334.

Birks, H.J.B., Heiri, O., Seppä, H., Bjune, A.E., 2010. Strengths and weaknesses of quantitative climate reconstructions based on Late-Quaternary biological proxies. The Open Ecology Journal 3, 68–110.

Birks, H.J.B., 1998. Numerical tools in palaeolimnology – progress, potentialities, and problems. Journal of Paleolimnology 20, 307–332.

Birks, H.J.B., 2012. Overview of numerical methods in Palaeolimnology. In: Birks, H.J.B., Lotter, A.F., Juggins, S., Smol, J.P. (Eds.), Data Handling and Numerical Techniques, vol. 5. Springer, Dordrecht, pp. 19–92.

Boelcke, O., Moore, D.M., Roig, F.A. (Eds.), 1985. Transeta Botánica de la Patagonia.

Delmonte, B., Andersson, P.S., Hansson, M., Schönberg, H., Petit, J.R., Basile-Doelsch, I., Maggi, V., 2008. Aeolian dust in East Antarctica (EPICA-Dome C and Vostok): provenance during glacial ages over the last 800 kyr. Geophysical Research Letters 35, L07703. http://dx.doi.org/10.1029/2008GL033382.

Endlicher, W., 1993. Klimatische Aspekte der Weidedegradation in Ost-Patagonien. In: Hornetz, B., Zimmer, D. (Eds.), Beiträge zur Kultur- und Regionalgeographie. Festschrift für Ralph Jätzold. Geographische Gesellschaft Trier, Trier, pp. 91–103.

Fletcher, M.-S., Moreno, P.I., 2012. Have the Southern Westerlies changed in a zonally symmetric manner over the last 14,000 years? A hemisphere-wide take on a controversial problem. Quaternary International 253, 32–46.

Gebhardt, A.C., De Batist, M., Niessen, F., Anselmetti, F.S., Ariztegui, D., Haberzettl, T., Kopsch, C., Ohlendorf, C., Zolitschka, B., 2011a. Deciphering lake and maar geometries from seismic refraction and reflection surveys in Laguna Potrok Aike (southern Patagonia, Argentina). Journal of Volcanology and Geothermal Research 201, 357–363.

Gebhardt, A.C., Ohlendorf, C., Niessen, F., De Batist, M., Anselmetti, F.S., Ariztegui, D., Kliem, P., Wastegård, S., Zolitschka, B., 2011b. Seismic evidence of up to 200 m lake-level change in Southern Patagonia since Marine Isotope Stage 4. Sedimentology. http://dx.doi.org/10.1111/j.1365–3091.2011.01296.x.

Gilli, A., Ariztegui, D., Anselmetti, F., Mc Kenzie, J., Markgraf, V., Hajdas, I., Mc Culloch, R., 2005. Mid-Holocene strengthening of the Southern Westerlies in South America. Sedimentological evidences from Lago Cardiel, Argentina (49°S). Global and Planetary Change 49, 75–93.

Grimm, E., 1987. CONISS: a fortran 77 program for stratigraphically constrained cluster analysis by the method of incremental sum of squares. Computers & Geosciences 13, 13–35.

Haberzettl, T., Fey, M., Lücke, A., Maidana, N.I., Mayr, C., Ohlendorf, C., Schäbitz, F., Schleser, G.H., Wille, M., Zolitschka, B., 2005. Climatically induced lake level changes during the last two millennia as reflected in sediments of Laguna Potrok Aike, southern Patagonia (Santa Cruz, Argentina). Journal of Paleolimnology 33, 283–302.

Haberzettl, T., Wille, M., Fey, M., Janssen, S., Lücke, A., Mayr, C., Ohlendorf, C., Schäbitz, F., Schleser, G.H., Zolitschka, B., 2006. Environmental change and fire history of southern Patagonia (Argentina) during the last five centuries. Quaternary International 158, 72–82.

Haberzettl, T., Corbella, H., Fey, M., Janssen, S., Lücke, A., Mayr, C., Ohlendorf, C., Schäbitz, F., Schleser, G.H., Wille, M., Wulf, S., Zolitschka, B., 2007. Wet–dry cycles in southern Patagonia – chronology, sedimentology and geochemistry of a lacustrine sediment record from Laguna Potrok Aike (Argentina). The Holocene 17 (3), 297–310.

Haberzettl, T., Kück, B., Wulf, S., Anselmetti, F., Ariztegui, D., Corbella, H., Fey, M., Janssen, S., Lücke, A., Mayr, C., Ohlendorf, C., Schäbitz, F., Schleser, G.H., Wille, M., Zolitschka, B., 2008. Hydrological variability in southeastern Patagonia and explosive volcanic activity in the southern Andean Cordillera during Oxygen Isotope Stage 3 and the Holocene inferred from lake sediments of Laguna Potrok Aike, Argentina. Palaeogeography, Palaeoclimatology, Palaeoecology 259 (2–3), 213–229.

Haberzettl, T., Anselmetti, F.S., Bowen, S.W., Fey, M., Mayr, C., Zolitschka, B., Ariztegui, D., Mauz, B., Ohlendorf, C., Kastner, S., Lücke, A., Schäbitz, F., Wille, M., 2009. Late Pleistocene dust deposition in the Patagonian steppe – extending and refining the paleoenvironmental and tephrochronological record from Laguna Potrok Aike back to 55 ka. Quaternary Science Reviews 28, 2927–2939.

Hahn, A., Kliem, P., Ohlendorf, C., Zolitschka, B., Rosen, P., The PASADO Science Team, 2013. Climate induced changes in the carbonate and organic content of Laguna Potrok Aike sediments during the past 50 ka inferred from infrared spectroscopy. Quaternary Science Reviews 71, 154–166.

Herzschuh, U., Birks, H.J.B., Mischke, S., Zhang, C., Böhner, J., 2009. A modern pollen–climate calibration set from the eastern Tibetan Plateau and its application to a Late Quaternary pollen record from the Qilian Mountains. Journal of Biogeography 37 (4), 752–766. http://dx.doi.org/10.1111/j.1365-2699.2009.02245.x.

Heusser, C.J., 1971. Pollen and Spores of Chile. The University of Arizona Press, Tucson, Arizona.

Heusser, C.J., 1995. Three Late Quaternary pollen diagrams from Southern Patagonia and their palaeoecological implications. Palaeogeography, Palaeoclimatology, Palaeoecology 118, 1–24.

Heusser, C.J., 2003. Ice Age Southern Andes: a Chronicle of Paleoecological Events. Elsevier B.V., Amsterdam, The Netherlands.

Jouzel, J., Masson-Delmotte, V., Cattani, O., Dreyfus, G., Falourd, S., Hoffmann, G., Minster, B., Nouet, J., Barnola, J.M., Chappellaz, J., Fischer, H., Gallet, J.C., Johnsen, S., Leuenberger, M., Loulergue, L., Luethi, D., Oerter, H., Parrenin, F., Raisbeck, G., Raynaud, D., Schilt, A., Schwander, J., Selmo, E., Souchez, R., Spahni, R., Stauffer, B., Steffensen, J.P., Stenni, B., Stocker, T.F., Tison, J.L., Werner, M., Wolff, E.W., 2007. Orbital and millennial antarctic climate variability over the past 800,000 years. Science 317, 793–796.

Juggins, S., 2003. User Guide C2 – a Program for Analysing and Visualising Palaeoenvironmental Data. Department of Geography, University of Newcastle, UK.

Kaplan, M.R., Fogwill, C.J., Sugden, D.E., Hulton, N.R.J., Kubik, P.W., Freeman, S.P.H.T., 2008a. Southern Patagonian and Southern Ocean climate during the Last Glacial period. Quaternary Science Reviews 27, 284–294.

Kaplan, M.R., Moreno, P.I., Rojas, M., 2008b. Glacial dynamics in southernmost South America during Marine Isotope Stage 5e to the Younger Dryas chron: a brief review with a focus on cosmogenic nuclide measurements. Quaternary Research 23, 649–658.

Kilian, R., Lamy, F., 2012. A review of Glacial and Holocene paleoclimate records from southernmost Patagonia (49–55°S). Quaternary Science Reviews 53, 1–23.

Kilian, R., Schneider, C., Koch, J., Fesq-Martin, M., Biester, H., Casassa, G., Arevalo, M., Wendt, G., Baeza, O., Behrmann, J., 2006. Palaeoecological constraints on Late Glacial and Holocene ice retreat in the Southern Andes (53°S). Global and Planetary Change 59, 49–66.

Kliem, P., Buylaert, J.P., Hahn, A., Mayr, C., Ohlendorf, C., Wastegard, S., Zolitschka, B., 2013a. Geomorphological evidence and magnitude of lake-level oscillations at Laguna Potrok Aike, Patagonian steppe (Argentina). Quaternary Science Reviews 71, 131–146.

Kliem, P., Enters, D., Hahn, A., Ohlendorf, C., Wastegård, S., Zolitschka, B., The PASADO Science Team, 2013b. Lithology, absolute dating and hydrological interpretation of a 51,000 year old lacustrine record, Laguna Potrok Aike (Patagonia). Quaternary Science Reviews 71, 54–69.

Lamy, F., Kilian, R., Arz, H.W., Francois, J.-P., Kaiser, J., Prange, M., Steinke, T., 2010. Holocene changes in the position and intensity of the southern westerly wind belt. Nature Geoscience 3, 695–699.

Leemans, R., Cramer, W.P., 1991. The IIASA Database for Mean Monthly Values of Temperature, Precipitation and Cloudiness of the Global Terrestrial Grid. International Institute of Applied Systems Analyses, Laxenburg, Austria.

Legendre, P.L., Birks, H.J.B., 2012. From classical to canonical ordination. In: Birks, H.J.B., Lotter, A.F., Juggins, S., Smol, J.P. (Eds.), Tracking Environmental Change Using Lake Sediments. Data Handling and Numerical Techniques, vol. 5. Springer, Dordrecht, pp. 201–248.

Legendre, P., Gallagher, E., 2001. Ecologically meaningful transformations for ordination of species data. Oecologia 129 (2), 271–280.

Mancini, M., Paez, M., Prieto, A., 2002. Cambios ambientales durante los últimos 7.000 ^{14}C años en el ecotono bosque-estepa, 47°–48°S, Santa Cruz, Argentina. Ameghiniana 39 (2), 151–162.

Mancini, M.V., Prieto, A.R., Paez, M.M., Schäbitz, F., 2008. Late Quaternary vegetation and climate of Patagonia. In: Rabassa, J. (Ed.), Late Cenozoic of Patagonia and Tierra del Fuego, pp. 351–367.

Mancini, M.V., 1993. Recent pollen spectra from forest and steppe of South Argentina: a comparison with vegetation and climate data. Review of Palaeobotany and Palynology 77.

Mancini, M.V., 1998. Vegetational changes during the Holocene in the Extra-Andean Patagonia, Argentina. Palaeogeography, Palaeoclimatology, Palaeoecology 138, 207–219.

Mancini, M., 2002. Vegetation and climate during the Holocene in Southwest Patagonia, Argentina. Review of Palaeobotany and Palynology 122, 101–115.

Mancini, M.V., 2009. Holocene vegetation and climate changes from a peat pollen record of the forest – steppe ecotone, Southwest of Patagonia (Argentina). Quaternary Science Reviews 28, 1490–1497.

Markgraf, V., D'Antoni, H.L., 1978. Pollen Flora of Argentina. The University of Arizona Press, Tucson.

Markgraf, V., Huber, U., 2010. Late and postglacial vegetation and fire history in Southern Patagonia and Tierra del Fuego. Palaeogeography, Palaeoclimatology, Palaeoecology 297, 351–366. http://dx.doi.org/10.1016/j.palaeo.2010.08.013.

Markgraf, V., Bradbury, P., Schwalb, A., Burns, S., Stern, Ch., Ariztegui, D., Gilli, A., Anselmetti, F., Stine, S., Maidana, N., 2003. Holocene palaeoclimates of southern Patagonia: limnological and environmental history of Lago Cardiel, Argentina. The Holocene 13, 581–591.

Markgraf, V., 1993. Paleoenvironments and paleoclimates in Tierra del Fuego and southernmost Patagonia, South America. Palaeogeography, Palaeoclimatology, Palaeoecology 102, 53–68.

Mayr, C., Wille, M., Haberzettl, T., Fey, M., Janssen, S., Lücke, A., Ohlendorf, C., Oliva, G., Schäbitz, F., Schleser, G., Zolitschka, B., 2007a. Holocene variability of the Southern Hemisphere westerlies in Argentinean Patagonia (52°S). Quaternary Science Reviews 26, 579–584.

Mayr, C., Lücke, A., Stichler, W., Trimborn, P., Ercolano, B., Oliva, G., Ohlendorf, C., Soto, J., Fey, M., Haberzettl, T., Janssen, S., Schäbitz, F., Schleser, G.H., Wille, M., Zolitschka, B., 2007b. Precipitation origin and evaporation of lakes in semi-arid Patagonia (Argentina) inferred from stable isotopes (δ^{18}O, δ^{2}H). Journal of Hydrology 334, 53–63.

Mayr, C., Lücke, A., Maidana, N.I., Wille, M., Haberzettl, T., Corbella, H., Ohlendorf, C., Schäbitz, F., Fey, M., Janssen, S., Zolitschka, B., 2009. Isotopic fingerprints on lacustrine organic matter from Laguna Potrok Aike (southern Patagonia, Argentina) reflect environmental changes during the last 16,000 years. Journal of Paleolimnology 42, 81–102. http://dx.doi.org/10.1007/s10933-008-9249-8.

Mc Culloch, R.D., Bentley, M.J., Purves, R.S., Hulton, N.R.J., Sugden, D.E., Clapperton, C.M., 2000. Climatic inferences from glacial and palaeoecological evidence at the Last Glacial termination, southern South America. Journal of Quaternary Science 15 (4), 409–417.

Mendes, M.C.D., Trigo, R.M., Cavalcanti, I.F.A., DaCamara, C.C., 2008. Blocking episodes in the southern hemisphere: impact on the climate of adjacent continental areas. Pure and Applied Geophysics 165, 1941–1962.

Moreno, P., Francois, J.P., Moy, C.M., Villa-Martinez, R., 2010. Covariability of the Southern Westerlies and atmospheric CO_2 during the Holocene. Geology 38 (8), 727–730. http://dx.doi.org/10.1130/G30962.1.

Moy, C.M., Moreno, P.I., Dunbar, R.B., Kaplan, M.R., Francois, J.-P., Villalba, R., Haberzettl, T., 2009. Climate change in Southern South America during the last two millennia. In: Vimeux, F., Sylvestre, F., Khodri, M. (Eds.), Past Climate Variability in South America and Surrounding Regions, from the Last Glacial Maximum to the Holocene. Springer, pp. 353–394.

NGRIP-Members (North Greenland Ice Core Project Members), 9 September 2004. High-resolution record of Northern Hemisphere climate extending into the Last Interglacial period. Nature 431 (7005), 147–151.

Ohlendorf, C., Fey, M., Gebhard, C., Haberzettl, T., Lücke, A., Mayr, C., Schäbitz, F., Wille, M., Zolitschka, B., 2013. Mechanisms of lake-level change at Laguna Potrok Aike (Argentina) – insights from hydrological balance calculations. Quaternary Science Reviews 71, 27–45.

Overpeck, J.T., Webb, I.T., Prentice, I.C., 1985. Quantitative interpretation of fossil pollen spectra: dissimilarity coefficients and the method of modern analogs. Quaternary Research 23, 87–108.

Pedro, J.B., van Ommen, T.D., Rasmussen, S.O., Morgan, V.I., Chappellaz, J., Moy, A.D., Masson-Delmotte, V., Delmotte, M., 2011. The last deglaciation: timing the bipolar seesaw. Climate of the Past Discussions 7, 397–430. http://dx.doi.org/10.5194/cpd-7-397-2011.

Prieto, A.R., Stutz, S., Pastorino, S., 1998. Vegetación del Holoceno en la cueva Las Buitreras, Santa Cruz, Argentina. Revista Chilena de Historia Natural 71, 277–290.

Quintana, F.A., 2009. Paleoambietes del extremo sur de Santa Cruz: analisis polinico de sedimentos lacustres del Cuaternario tardio. Ph.D. thesis, Fac. Cienc. Exactas Nat. Univ. Nac. Mar del Plata, Argentina, 146 pp.

Schäbitz, F., Paez, M.M., Mancini, M.V., Quintana, F.A., Wille, M., Corbella, H., Haberzettl, T., Lücke, A., Prieto, A.R., Maidana, N.I., Mayr, C., Ohlendorf, C., Schleser, G.H., Zolitschka, B., 2003. Estudios paleoambientales en lagos volcánicos en la Región Volcánica de Pali Aike, sur de Patagonia (Argentina): palinología. Revista del Museo Argentino de Ciencias Naturales, Nueva Serie 5 (2), 301–316.

Schäbitz, F., 1999. Paläoökologische Untersuchungen an geschlossenen Hohlformen in den Trockengebieten Patagoniens. Bamberger Geographische Schriften, Heft 17.

Schneider, C., Glaser, M., Kilian, R., Santana, A., Butorovic, N., Casassa, G., 2002. Weather observations across the southern Andes at 53°S. Physical Geography 24, 97–119.

Schwerdtfeger, W. (Ed.), 1976. Climates of Central and South America. World Survey of Climatology, vol. 12. Elsevier, Amsterdam, Oxford, New York.

Seluchi, M.E., Norte, F.A., Satyamurty, P., Chou, S.C., 2003. Analysis of three situations of the Foehn effect over the Andes (Zonda Wind) using the Eta–CPTEC regional model. Weather and Forecasting 18, 481–501.

Seppä, H., Birks, H.J.B., Odland, A., Poska, A., Veski, S., 2004. A modern pollen–climate calibration set from northern Europe: developing and testing a tool for palaeoclimatological reconstructions. Journal of Biogeography 31, 251–267.

Tonello, M.S., Mancini, M.V., Seppä, H., 2009. Quantitative reconstruction of Holocene precipitation changes in southern Patagonia. Quaternary Research 72, 410–420.

Villa-Martínez, R., Moreno, P.I., 2007. Pollen evidence for variations in the southern margin of the westerly winds in SW Patagonia over the last 12,600 years. Quaternary Research 68, 400–409.

Wagner, S., Widmann, M., Jones, J., Haberzettl, T., Lücke, A., Mayr, C., Ohlendorf, C., Schäbitz, F., Zolitschka, B., 2007. Transient simulations, empirical reconstructions and forcing mechanisms for the Mid-Holocene hydrological climate in Southern Patagonia. Climate Dynamics 29, 333–355.

Weischet, W., 1996. Regionale Klimatologie. Teil 1: Die Neue Welt (Amerika, Neuseeland, Australien). Teubner, Stuttgart.

Wille, M., Schäbitz, F., 2009. Late Glacial and Holocene climate dynamics at the steppe-forest ecotone in southernmost Patagonia: the pollen record from a swamp near Brazo Sur, Lago Argentino. Vegetation History and Archaeobotany 18, 225–234.

Wille, M., Maidana, N.I., Schäbitz, F., Fey, M., Haberzettl, T., Janssen, S., Lücke, A., Mayr, C., Ohlendorf, C., Schleser, G.H., Zolitschka, B., 2007. Vegetation and climate dynamics in southern South America: the microfossil record of Laguna Potrok Aike, Santa Cruz, Argentina. Review of Palaeobotany and Palynology 146, 234–246.

Xu, Q., Li, Y., Bunting, M.J., Tian, F., Liu, J., 2010. The effects of training set selection on the relationship between pollen assemblages and climate parameters: implications for reconstructing past climate. Palaeogeography, Palaeoclimatology, Palaeoecology 289 (1–4), 123–133.

Zolitschka, B., Schäbitz, F., Lücke, A., Corbella, H., Ercolano, B., Fey, M., Haberzettl, T., Janssen, S., Maidana, N.I., Mayr, C., Ohlendorf, C., Oliva, G., Paez, M.M., Schleser, G.H., Soto, J., Tiberi, P., Wille, M., 2006. Palaeoecological potential of crater lakes in the Pali Aike Volcanic Field, southern Patagonia (Argentina). Journal of South American Earth Sciences 21, 294–309.